Mesoporous Nanospheres

DOI: 10.1002/anie.201402002

Dual-Pore Mesoporous Carbon@Silica Composite Core–Shell Nanospheres for Multidrug Delivery**

*Yin Fang, Gengfeng Zheng, Jianping Yang, Haosha Tang, Yafeng Zhang, Biao Kong, Yingying Lv, Congjian Xu, Abdullah M. Asiri, Jian Zi, Fan Zhang, and Dongyuan Zhao**

Abstract: *Monodispersed mesoporous phenolic polymer nanospheres with uniform diameters were prepared and used as the core for the further growth of core–shell mesoporous nanorattles. The hierarchical mesoporous nanospheres have a uniform diameter of 200 nm and dual-ordered mesopores of 3.1 and 5.8 nm. The hierarchical mesostructure and amphiphilicity of the hydrophobic carbon cores and hydrophilic silica shells lead to distinct benefits in multidrug combination therapy with cisplatin and paclitaxel for the treatment of human ovarian cancer, even drug-resistant strains.*

Mesoporous materials have diverse applications in catalysis, energy storage, separation, and biomedicine due to their unique properties attributed to high surface area, large pore volume, and regular large pore size.[1–6] Through the control of the growth and cooperation–assembly processes in solution phase, the morphology and particle size of the products can be modified. One important and exciting advance is to fabricate nanosized particles with ordered mesostructures through controlled sol–gel procedures in solution phase.[7–16] These mesostructured nanoparticles are attractive since they combine the advantages of the quantum effect of nanosized particles and the high surface area of mesostructures, which can lead to unconventional properties.

[*] Y. Fang, Prof. G. Zheng, J. Yang, B. Kong, Y. Lv, Prof. F. Zhang, Prof. D. Zhao
Department of Chemistry and Shanghai Key Lab of Molecular Catalysis and Innovative Materials
State Key Laboratory of Molecular Engineering of Polymers and Advanced Materials Laboratory
Fudan University, Shanghai 200433 (P.R. China)
E-mail: dyzhao@fudan.edu.cn
H. Tang, Prof. C. Xu
Obstetrics and Gynecology Hospital of Fudan University (China)
Y. Zhang, Prof. J. Zi
Department of Physics, Fudan University (China)
Prof. A. M. Asiri
Chemistry Department and The Center of Excellence for Advanced Materials Research, King Abdulaziz University (Saudi Arabia)

[**] This work was supported by the Key Basic Research Program (973 Project) (2013CB934104, 2012CB224805), the NSFC (21101029, 21273041, 21210004, 21322311), the State Key Laboratory of Pollution Control and Resource Reuse Foundation (PCRRF12001), Science & Technology Commission of Shanghai Municipality (08DZ2270500), Shanghai Key Laboratory of Molecular Catalysis and Innovative Materials, and King Abdulaziz University (KAU) (grant no. 32-3-1432/HiCi).

Supporting information for this article is available on the WWW under http://dx.doi.org/10.1002/anie.201402002.

Recently, substantial research efforts have been made to fabricate multifunctional mesoporous nanospheres by designing multicompartment compositions and constructing hierarchical porous structures.[17–22] The local variables in single nanospheres can be approached by modifying the physical/chemical properties of the pore environments. For example, Wiesner and co-workers prepared a class of ordered mesoporous silica nanospheres (MSNs) containing both cubic and hexagonal mesostructured compartments within one particle by means of the epitaxial growth of hexagonal silica on the cubic nanospheres.[20] Qiao et al. reported the synthesis of core–shell-structured mesoporous nanospheres with two sets of mesopores by sol–gel coating and a selective etching prodecure.[19]

Multifunctional mesoporous nanospheres have been demonstrated to be excellent nanocarriers in drug delivery.[23–29] Most of these nanocarriers are mainly based on mesoporous silica nanospheres, which are biocompatible and hydrophilic but have poor affinity with hydrophobic drug molecules. However, anticancer drugs show various affinities in chemotherapy: 40% of them are hydrophobic and the rest (60%) are hydrophilic.[30] The variety of affinities may affect multidrug loading and delivery by the mesoporous nanocarriers. Thus, the design and fabrication of mesoporous nanostructures with hydrophilic/hydrophobic amphiphilicity and dual-pore channels is necessary for the development of improved drug-delivery systems. However, to the best of our knowledge, the synthesis of non-silica hierarchical mesoporous nanostructures is still a big challenge.[13,15] Moreover, the fabrication of multimodal hierarchical mesostructures with hybrid compositions and amphiphilicity in one single nanoparticle has not been demonstrated yet.

Herein we report the synthesis of a novel type of uniform dual-pore mesoporous, hierarchical carbon@silica core–shell nanospheres for the first time, by an in situ coating method. Monodispersed mesoporous polymer nanospheres are first prepared by a low-concentration hydrothermal treatment. These uniform nanospheres are suitable building blocks for constructing hierarchical nanostructures. The hydrophilic polymer nanospheres are employed as a core and coated with a uniform layer of mesoporous silica by a surfactant-templated sol–gel method. The key point is that the as-prepared hydrophilic polymer nanospheres are suitable for in situ coating; they can be easily tuned into hydrophobic mesoporous carbon nanospheres by a subsequent carbonization procedure (synthesis scheme is shown in the Supporting Information). The obtained core–shell mesoporous nanospheres display a uniform rattle-like morphology and hierarchical dual-pore mesostructure with pores that are 3.1 and

5.8 nm in diameter. Using human ovarian cancer cells as a model, we demonstrated that these dual-pore mesoporous nanoparticles efficiently load hydrophilic cisplatin and hydrophobic paclitaxel multidrugs,[31–34] and kill drug-resistant human ovarian cancer cells with high efficacy.

The monodispersed as-made mesoporous polymer nanospheres, which were synthesized by using Pluronic F127 as a template and phenol/formaldehyde as a precursor serve as the starting core. The obtained colloid products display good dispersity in water even after storage for several weeks (Figure 1 a). The khaki color of the colloid spheres may be

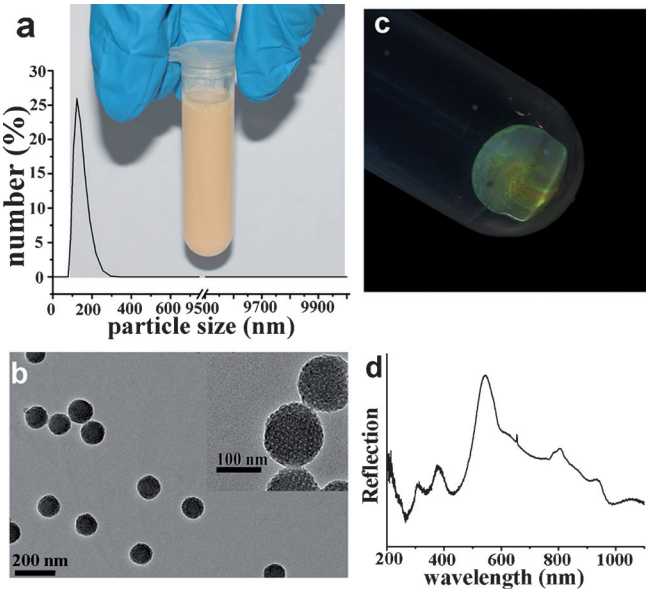

Figure 1. a) Photograph of a sample of the mesoporous polymer colloid and the DLS particle size distribution (inset). b) TEM image of the mesoporous polymer colloid spheres. c) Photograph and d) reflection spectrum of the mesoporous colloid phenolic resin polymer spheres under normal incidence light after centrifugation and removal of supernatant.

caused from the cross-linking and partial oxidation of phenolic resins. Dynamic light scattering (DLS) demonstrates that the polydispersity index (PDI) of the mesoporous polymer nanospheres is roughly 1 %, indicating the monodispersity of the colloid particles. The TEM image (Figure 1 b) shows that these colloidal nanospheres have a uniform particle size of about 120 nm and the ordered mesostructures is evident (Figure 1 b inset). The good uniformity and monodispersity of the mesoporous polymer colloid nanospheres can be further confirmed by the light reflection after centrifugation of the products. The product deposited on the bottom of the centrifuge tube displays a bright iridescent green color (Figure 1 c). The spectrum of the colloidal nanospheres under normal incidence light shows several distinct peaks, including a sharp peak centered at around 550 nm in the visible region in accordance with the perceived color (Figure 1 d).[35–37] The mesoporous polymer nanospheres are uniform enough to form a novel type of mesoporous photonic crystals by the self-assembly; this unique phenomenon is observed for the first time as far as we know. These results clearly suggest the formation of a photonic crystal structure from the ordered closed-packing of the nanosphere samples, indicating a highly uniform particle size. Furthermore, the synthesis of the mesoporous nanospheres can be scaled up easily without apparent limitation.

After calcination at 600 °C in N_2 atmosphere, the monodispersed mesoporous polymer nanospheres are carbonized. SEM images show that the obtained mesoporous carbon nanospheres have uniform distribution in both particle size and morphology; the diameter (ca. 100 nm) is smaller than that of the mesoporous polymer nanospheres (Figure 2 a–d and Figure S1). The uniformity of mesoporous carbon nano-

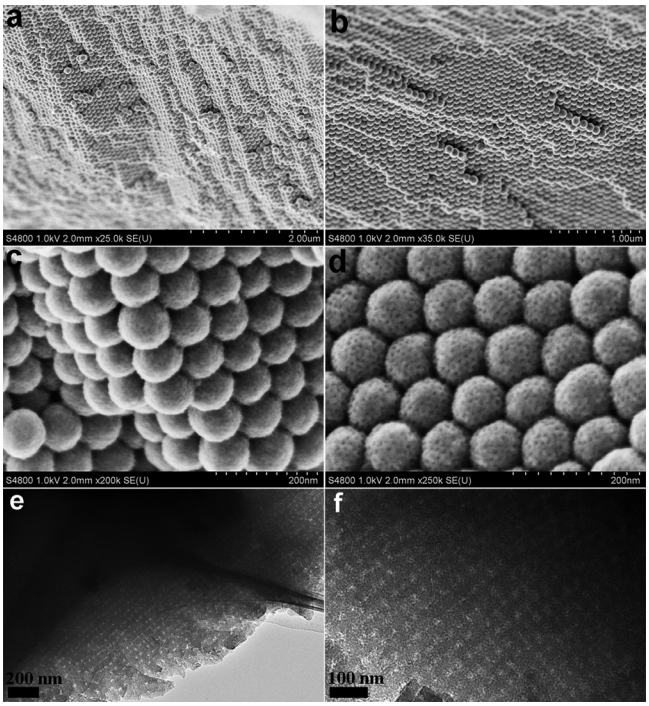

Figure 2. SEM (a–d) and TEM (e, f) images of the ordered close-packed structures of the monodispersed mesoporous carbon nanospheres calcinated at 600 °C in N_2.

spheres enables their self-assembly into an ordered close-packed face-centered-cubic (fcc) structure, from which the uniform mesopores on the surface of each carbon nanosphere are clearly observed (Figure 2 c,d). The TEM images exhibit interparticle texture between mesoporous carbon nanospheres with uniform pore sizes of 20 nm. They have a highly ordered arrangement, confirming the close-packed structure of the monodispersed mesoporous carbon nanospheres (Figure 2 e,f and Figure S1 d).

The monodispersed mesoporous polymer (MP) nanospheres with a diameter of 120 nm can be further coated with a layer of nonporous silica shells ($nSiO_2$) in Stöber solution. SEM images of the resultant MP@$nSiO_2$ samples display spherical and uniform core–shell structures, with an increased diameter of 180 nm (Figure 3 a). The uniform core–shell structure is further illustrated by TEM images. A layer of

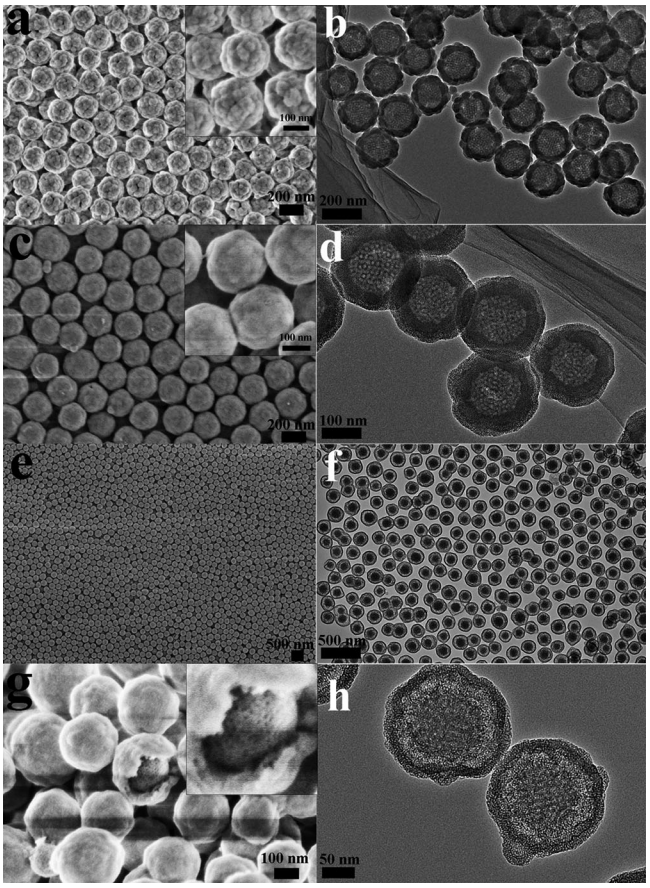

Figure 3. SEM (a, c, e) and TEM (b, d, f) images of the core–shell-structured nanospheres prepared by using mesoporous polymer as cores; a, b) the mesoporous polymer@condensed silica (MP@nSiO_2); c, d) mesoporous polymer@condensed silica@mesoporous silica (MP@nSiO_2@MS); e, f) the rattlelike core–shell mesoporous polymer@mesoporous silica (MP@MS) structure after the middle condensed silica layer had been etched; highly uniform nanospheres in a large domain are visible; g, h) high-resolution SEM and TEM images of the mesoporous carbon@mesoporous silica nanospheres (MC@MS) after calcination at 600 °C, showing the rattlelike dual-pore mesoporous structures.

a roughly 30 nm-thick amorphous silica shell coated on the phenolic polymer cores is clearly observed (Figure 3 a,b), which consists of dozens of protuberant silica nanoparticles (Figure 3 a inset and 3 b). The MP@nSiO_2 nanospheres can be coated further with a layer of mesoporous silica by the surfactant-assisted sol–gel process in ammonia solution. SEM images show that the core–shell MP@nSiO_2@MS structures also have a uniform spherical morphology with a relatively monodisperse size distribution of 210 nm (Figure 3 c). The hierarchical sandwich structure of these MP@nSiO_2@MS nanospheres is clearly evident in TEM images (Figure 3 d). The structure includes a uniform mesoporous polymer core roughly 120 nm in diameter, covered by 30 nm-thick amorphous, nonporous silica as an intermediate layer, and then a 15 nm-thick mesoporous silica shell. Finally, after selective etching of the intermediate amorphous silica layer by weak alkaline solution, a uniform rattlelike core–shell nanostructure is obtained (Figure 3 e,f). The spacing between the inner phenolic cores and the outer mesoporous silica shells is measured to be roughly 30 nm, corresponding well to the thickness of the amorphous silica layer, further suggesting that the condensed silica layer can be selectively removed by Na_2CO_3 solution. After calcination at 600 °C in N_2 atmosphere, the inner polymer core is carbonized. The SEM images obtained from some cracked spheres clearly show the cavities between the core and shell, further confirming the rattlelike MC@MS nanostructure. High-resolution SEM images also display the open and accessible mesopores on the surface of the inner cores (Figure 3 g). TEM images also show that the inner carbon cores have ordered mesostructures, which are completely encapsulated in the cavities (Figure 3 h, and Figure S2 a,b). Furthermore, the TEM images of the mesoporous carbon nanospheres recorded after the mesoporous silica shells had been etched off also clearly show the ordered mesopores, which further confirm the ordered mesostructures of the inner cores (Figure S2 c). The hierarchical dual-pore mesostructure of the rattlelike mesoporous carbon MC@MS samples is also demonstrated by the N_2 sorption isotherms. Density function theory (DFT) calculations from the N_2 sorption isotherms (based on a carbon slit pore model) confirm the existence of 5.8 nm pores, which are derived from the mesoporous carbon cores, while the broadened peak from 2.5 to 3.7 nm indicates the existence of mesopores on the mesoporous SiO_2 shells (Figure S3, more detail in the Supporting Information). However, the small-angle X-ray scattering (SAXS) integral curves of the MC@MS samples show a weak and broad scattering peak at a q value of roughly 0.75 nm^{-1} (Figure S4), perhaps due to the nanosized ordered mesoporous carbon domains and the shielding effect of the X-ray radiation by the mesoporous silica shells.

The permeability of the obtained dual-pore mesoporous MC@MS nanospheres into cells was investigated by using fluorescein isothiocyanate (FITC) as a tracer. The confocal laser scanning microscope (CLSM) images of SKOV3 cells display a remarkable intracellular luminescence (Figure 4 a–c). The overlaid images show that the luminescence is observed from the cytoplasm of the cells, implying the successful uptake of the dual-pore mesoporous MC@MS nanospheres into the living cells. Because of the hydrophilic/hydrophobic amphiphilicity of the rattlelike dual-pore mesoporous nanospheres, multidrugs with hydrophilic or/and hydrophobic properties could be loaded into the nanospheres. Only a few examples of nanocarriers encapsulating hydrophilic drugs along with hydrophobic drugs have been reported, in fact, which is quite difficult for the pure mesoporous silica nanospheres (MSN).[30]

We selected hydrophobic paclitaxel (Ptxl) and hydrophilic cisplatin as model drugs, which are commonly combined in treatments of human ovarian cancer cells.[31–34] The loading amounts of paclitaxel and cisplatin drugs in the duel-pore mesoporous nanospheresare 10.2 % and 12.6 %, respectively (see the Supporting Information), indicating the efficient encapsulation of both paclitaxel and cisplatin drugs. The cell viability was further measured by the Cell Counting Kit-8 (CCK-8) assays (Figure 4 d,e). Over 90 % of the cells (both SKOV3 and A2780 (CP70) cells) are still alive after being cultured with 50 $\mu g\,mL^{-1}$ of the dual-pore mesoporous

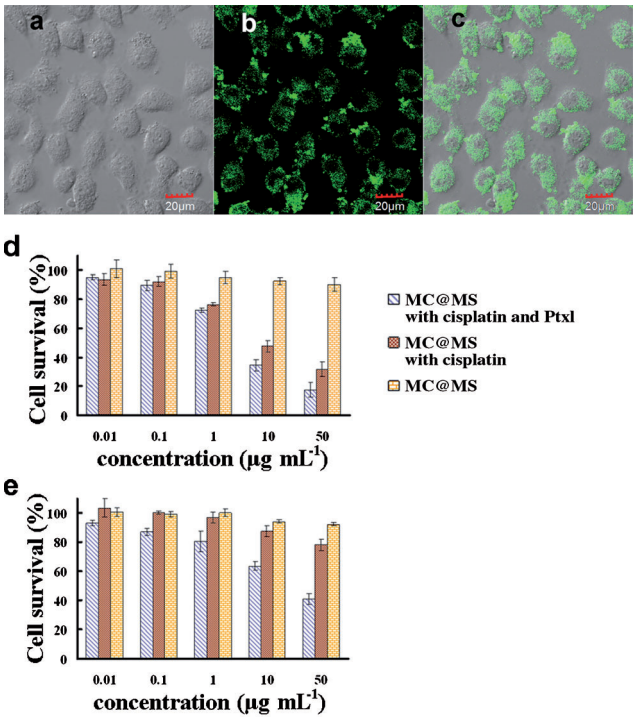

Figure 4. Bright (a), fluorescence (b), and overlay CLSM images (c) of SKOV3 after incubation for 3 h with the rattlelike dual-pore mesoporous carbon/silica nanospheres MC@MS grafted with FITC group. d, e) Cytotoxicity of cisplatin and Ptxl drugs loaded into the MC@MS nanospheres, cisplatin alone loaded into MC@MS nanospheres, and dual-pore mesoporous MC@MS nanospheres at the same dose in different human ovarian cancer cells (d) normal ovarian cancer cells SKOV3, and (e) drug-resistant A2780 (CP70) cells.

carbon@silica nanospheres, indicating a low cell cytotoxicity. When SKOV3 cells were cultured with both the rattlelike MC@MS loaded with only cisplatin (denoted as MC@MS-Pt) and MC@MS loaded with both cisplatin and Ptxl (denoted as MC@MS-Pt-Ptxl), over 50% are killed, clearly indicating the good therapeutic effect of the nanocarriers loading with chemical drugs for the normal human ovarian cancer cells (Figure 4d). However, when drug-resistant cells were cultured with the sample MC@MS-Pt at a concentration of 50 $\mu g\,mL^{-1}$ for 24 h, over 80% of the cisplatin-resistant A2780 (CP70) cells are still alive (Figure 4e). When the same cells were cultured with 50 $\mu g\,mL^{-1}$ of the sample MC@MS-Pt-Ptxl for 24 h, over 50% of cisplatin-resistant cells are killed by the multidrug system. Therefore, the performance of the MC@MS-Pt-Ptxl drug nanocarriers are significantly enhanced over that of the single-drug-loaded MC@MS-Pt. These results clearly suggest that the therapeutic effect can substantially benefit from the multidrug combination system with the unique mesoporous structure.

In summary, we have reported a new strategy to synthesize a unique rattlelike dual-pore mesoporous carbon@silica hybrid nanospheres by using monodispersed resin polymer nanospheres with highly ordered mesostructures as cores and applying a surfactant-assistant sol–gel process. The obtained mesoporous rattlelike MC@MS nanospheres have a high surface area, large pore volume, very uniform diameter of roughly 200 nm, and dual mesopores of 3.1 and 5.8 nm. The hydrophobic mesoporous carbon cores have good affinity with water-insoluble drugs, while the hydrophilic mesoporous silica shells present good affinity with water-soluble drugs and significant biocompatibility. These hierarchical porous mesostructured MC@MS nanoparticles allow for efficient loading of typical multidrug-based combination therapy systems, and demonstrate effective inhibition of human ovarian cancer cells, with over 50% killing efficacy even for drug-resistant cells. Our discovery of the dual-pore mesoporous carbon@silica hybrid nanospheres may lead to further development of new concepts and architectures of nanocarriers, thus allowing for more opportunities in drug delivery and disease treatment.

Received: February 1, 2014
Published online: April 24, 2014

Keywords: core–shell structures · drug delivery · mesoporous materials · nanoparticles · photonic crystals

[1] Y. Wan, D. Zhao, *Chem. Rev.* **2007**, *107*, 2821.
[2] C. Liang, Z. Li, S. Dai, *Angew. Chem.* **2008**, *120*, 3754; *Angew. Chem. Int. Ed.* **2008**, *47*, 3696.
[3] Y. Zhai, Y. Dou, D. Zhao, P. F. Fulvio, R. T. Mayes, S. Dai, *Adv. Mater.* **2011**, *23*, 4828.
[4] Y. Fang, Y. Y. Lv, R. C. Che, H. Y. Wu, X. H. Zhang, D. Gu, G. F. Zheng, D. Y. Zhao, *J. Am. Chem. Soc.* **2013**, *135*, 1524.
[5] A. Stein, Z. Y. Wang, M. A. Fierke, *Adv. Mater.* **2009**, *21*, 265.
[6] A. H. Lu, S. Dai, *J. Mater. Chem. A* **2013**, *1*, 9326.
[7] Z. Li, J. C. Barnes, A. Bosoy, J. F. Stoddart, J. I. Zink, *Chem. Soc. Rev.* **2012**, *41*, 2590.
[8] I. Slowing, J. L. Vivero-Escoto, C. W. Wu, V. S. Lin, *Adv. Drug Delivery Rev.* **2008**, *60*, 1278.
[9] F. Tang, L. Li, D. Chen, *Adv. Mater.* **2012**, *24*, 1504.
[10] Y. Piao, A. Burns, J. Kim, U. Wiesner, T. Hyeon, *Adv. Funct. Mater.* **2008**, *18*, 3745.
[11] L. Pan, Q. He, J. Liu, Y. Chen, M. Ma, L. Zhang, J. Shi, *J. Am. Chem. Soc.* **2012**, *134*, 5722.
[12] D. P. Ferris, Y. L. Zhao, N. M. Khashab, H. A. Khatib, J. F. Stoddart, J. I. Zink, *J. Am. Chem. Soc.* **2009**, *131*, 1686.
[13] Y. Fang, D. Gu, Y. Zou, Z. Wu, F. Li, R. Che, Y. Deng, B. Tu, D. Zhao, *Angew. Chem.* **2010**, *122*, 8159; *Angew. Chem. Int. Ed.* **2010**, *49*, 7987.
[14] Z. A. Qiao, B. K. Guo, A. J. Binder, J. H. Chen, G. M. Veith, S. Dai, *Nano Lett.* **2013**, *13*, 207.
[15] A. Stein, B. E. Wilson, S. G. Rudisill, *Chem. Soc. Rev.* **2013**, *42*, 2763.
[16] T. Y. Yang, J. Liu, Y. Zheng, M. J. Monteiro, S. Z. Qiao, *Chem. Eur. J.* **2013**, *19*, 6942.
[17] Y. Yang, X. Liu, X. B. Li, J. Zhao, S. Y. Bai, J. Liu, Q. H. Yang, *Angew. Chem.* **2012**, *124*, 9298; *Angew. Chem. Int. Ed.* **2012**, *51*, 9164.
[18] F. Li, Z. Wang, A. Stein, *Angew. Chem.* **2007**, *119*, 1917; *Angew. Chem. Int. Ed.* **2007**, *46*, 1885; D. Niu, Z. Ma, Y. Li, J. Shi, *J. Am. Chem. Soc.* **2010**, *132*, 15144.
[19] J. Liu, S. Z. Qiao, S. B. Hartono, G. Q. Lu, *Angew. Chem.* **2010**, *122*, 5101; *Angew. Chem. Int. Ed.* **2010**, *49*, 4981.
[20] T. Suteewong, H. Sai, R. Hovden, D. Muller, M. S. Bradbury, S. M. Gruner, U. Wiesner, *Science* **2013**, *340*, 337.
[21] F. Han, D. Li, W. C. Li, C. Lei, Q. Sun, A. H. Lu, *Adv. Funct. Mater.* **2013**, *23*, 1692.

[22] A. H. Lu, T. Sun, W. C. Li, Q. Sun, F. Han, D. H. Liu, Y. Guo, *Angew. Chem.* **2011**, *123*, 11969; *Angew. Chem. Int. Ed.* **2011**, *50*, 11765.
[23] J. Liu, H. Q. Yang, F. Kleitz, Z. G. Chen, T. Y. Yang, E. Strounina, G. Q. Lu, S. Z. Qiao, *Adv. Funct. Mater.* **2012**, *22*, 591.
[24] R. Liu, P. H. Liao, J. K. Liu, P. Y. Feng, *Langmuir* **2011**, *27*, 3095.
[25] G. K. Such, A. P. Johnston, F. Caruso, *Chem. Soc. Rev.* **2011**, *40*, 19.
[26] Y. J. Wong, L. Zhu, W. S. Teo, Y. W. Tan, Y. Yang, C. Wang, H. Chen, *J. Am. Chem. Soc.* **2011**, *133*, 11422.
[27] R. Liu, Y. Zhang, X. Zhao, A. Agarwal, L. J. Mueller, P. Y. Feng, *J. Am. Chem. Soc.* **2010**, *132*, 1500.
[28] Y. Zhao, B. G. Trewyn, I. I. Slowing, V. S.-Y. Lin, *J. Am. Chem. Soc.* **2009**, *131*, 8398.
[29] R. Liu, Y. Zhang, P. Y. Feng, *J. Am. Chem. Soc.* **2009**, *131*, 15128.
[30] Q. He, M. Ma, C. Wei, J. Shi, *Biomaterials* **2012**, *33*, 4392.
[31] W. P. McGuire, W. J. Hoskins, M. F. Brady, P. R. Kucera, E. E. Partridge, K. Y. Look, D. L. Clarke-Pearson, M. Davidson, *New Eng. J. Med.* **1996**, *334*, 1.
[32] S. Aryal, C. M. Hu, L. Zhang, *Small* **2010**, *6*, 1442.
[33] B. Stordal, R. Davey, *Curr. Cancer Drug Targets* **2009**, *9*, 354.
[34] F. Ren, R. Chen, Y. Wang, Y. Sun, Y. Jiang, G. Li, *Pharm. Res.* **2011**, *28*, 897.
[35] S. Wang, W. C. Li, G. P. Hao, Y. Hao, Q. Sun, X. Q. Zhang, A. H. Lu, *J. Am. Chem. Soc.* **2011**, *133*, 15304.
[36] D. P. Josephson, E. J. Popczun, A. Stein, *J. Phys. Chem. C.* **2013**, *117*, 13585.
[37] C. I. Aguirre, E. Reguera, A. Stein, *Adv. Funct. Mater.* **2010**, *20*, 2565.

